Drug Delivery and Translational Research
https://doi.org/10.1007/s13346-020-00803-7

ORIGINAL ARTICLE

QbD aided development of ibrutinib-loaded nanostructured lipid carriers aimed for lymphatic targeting: evaluation using chylomicron flow blocking approach

Nagarjun Rangaraj[1] · Sravanthi Reddy Pailla[1] · Saurabh Shah[1] · Shubham Prajapati[1] · Sunitha Sampathi[1]

Abstract

Ibrutinib (IBR) is the choice of drug for the treatment of chronic lymphocytic leukaemia (CLL) and mantle cell lymphoma (MCL). IBR has low oral bioavailability of 2.9% owing to its high first pass metabolism. Present study was aimed to develop the nanostructured lipid carriers (NLC) using glyceryl monostearate (GMS) as solid lipid and Capryol™ PGMC as liquid lipid. Plackett-Burman design (PBD) was applied to screen the significant factors; furthermore, these significant factors were subjected to optimisation using Central Composite design (CCD). The size, poly dispersity index (PDI) and entrapment efficiency (E.E.) of the developed NLC were 106.4 ± 8.66 nm, 0.272 ± 0.005 and 70.54 ± 5.52% respectively. Morphological evaluation using transmission electron microscope (TEM) and field emission scanning electron microscope (FESEM) revealed spherical particles. Furthermore, differential scanning calorimetry (DSC) indicates the formation of molecular dispersion of drug in the melted lipid matrix while Powder X-Ray Diffraction (PXRD) studies reveal the absence of crystalline drug peaks in the formulation diffractogram. In-vivo pharmacokinetics of NLC displayed an increase in C_{max} (2.89-fold), $AUC_{0\text{-}t}$ (5.32-fold) and mean residence time (MRT) (1.82-fold) compared with free drug. Furthermore, lymphatic uptake was evaluated by chylomicron flow blocking approach using cycloheximide (CXI). The pharmacokinetic parameters C_{max}, $AUC_{0\text{-}t}$ and MRT of NLC without CXI were 2.75, 3.57 and 1.30 folds higher compared with NLC with CXI. The difference in PK parameters without CXI indicates significant lymphatic uptake of the formulation. Hence, NLC can be a promising approach to enhance the oral bioavailability of drugs with high first-pass metabolism.

Keywords Bioavailability enhancement · Central composite design · Cycloheximide · Ibrutinib · Multivariate analysis · Plackett-Burman design

Introduction

Ibrutinib (IBR), an irreversible Bruton's tyrosine kinase (BTK) inhibitor, is undoubtedly a breakthrough drug that has transformed the treatment of chronic lymphocytic leukaemia (CLL) and mantle cell lymphoma (MCL). CLL and MCL are common types of leukaemia in the western hemisphere. IBR belongs to type IV of irreversible kinase inhibitors and has a high potency (IC_{50} of 0.5 nM) and selectivity towards BTK, causing blockage of the B cell receptor (BCR) pathway [1–3]. Apart from the BTK, IBR displays variable binding affinities towards various kinases (TFK, EGFR family, BLK and JAK3); hence, various clinical trials are in progress to evaluate its efficiency in the treatment of other tumours. Though IBR has evolved as a promising drug in B cell malignancies, it suffers from poor oral bioavailability (BA) of only 2.9% which can be accounted for its low aqueous solubility (0.002 mg/mL) and high first-pass metabolism [4]. Consequently, the drug is available at high doses (daily dose of 560 mg and 420 mg for MCL and CLL respectively). The higher dose of the drug causes severe gastrointestinal bleeding, infections, decreased blood cell count ventricular arrhythmias, atrial fibrillation and atrial flutter [5, 6]. These adverse effects may be attenuated by dose reduction which can be brought about by ameliorating the BA. Hence, it is mandatory

Electronic supplementary material The online version of this article (https://doi.org/10.1007/s13346-020-00803-7) contains supplementary material, which is available to authorized users.

✉ Sunitha Sampathi
sunithaniper10@gmail.com

[1] Department of Pharmaceutics, National Institute of Pharmaceutical Education and Research, Hyderabad, Telangana 500037, India

Published online: 09 June 2020

to enhance its BA by minimizing the first-pass effect. In such an instance, it is obligatory to develop a formulation which maintains the drug's amorphous state and bypass the first-pass effect [7]. Therefore, lipid–aided drug delivery systems aimed to target absorption through the lymphatic system is a rational approach to enhance the bioavailability [8]. These lipid formulations improve the bioavailability of the drug by different mechanisms:

- Avoidance of solid-state problems: particle size reduction causes the drug to be available in a dispersed form into the lipid matrix thus preventing aggregation of drug molecules, crystal growth and other solid state manifestations easing the formation of solubilised phases and accelerating the dissolution process [9–12].
- Permeability glycoprotein (P-gp) efflux pump (that pumps external substances out of cells) can be circumvented by certain stabilisers like Pluronics®, D-α-tocopherol polyethylene glycol 1000 succinate (TPGS) [9].
- Lipids stimulate the enterocytes leading to an increased formation of chylomicrons which increase the lymph secretion. Lipid nanoparticles will form uni- or multilamellar vesicles in the presence of chylomicrons and get transported into lymph thus by-passing the first-pass metabolism leading to augmented oral bioavailability [13–15].

Approaches like self-nano emulsifying drug delivery system (SNEDDS), phospholipid complexes and co-amorphous systems [16] have been developed for the bioavailability enhancement of ibrutinib [4, 7]. The development of these formulations was done traditionally without the application of Quality by Design approach (QbD). Application of QbD provides an in-depth understanding of the interaction of various factors involved. Phospholipid complexes and emulsions are the traditional lipid formulations which are proven to be efficient but are limited by stability. Co-amorphous system was developed to overcome the low solubility, but not the first-pass effect [16]. Hence, it is advisable to use a lipid carrier system which can decrease first-pass effect by increasing the lymphatic uptake. One such system is solid lipid nanoparticles (SLNs) which are made of solid lipid(s) stabilised by one or more stabilisers in an aqueous phase [17]. SLNs possess several advantages like controlled release, tolerability (compared with polymeric nanoparticles) [18], scale-up feasibility [17] and can incorporate both hydrophilic and hydrophobic drugs [10, 19–21]. However, there are certain limitations such as poor drug loading, drug expulsion caused by lipid crystallisation and poor stability. To address these limitations, NLC have been developed which is similar to SLN in composition except for the addition of liquid lipid. Presence of liquid lipid causes amelioration in drug loading and also prevents the drug leakage as shown in supplementary Fig. 1 [22–24]. Hence, NLC are considered the next generation SLNs [18]. NLC are one of the most widely used lipid-based formulations which possess the combined advantages of nanotechnology and lipid emulsion systems [11]. The objective of this study was to investigate the efficacy of NLC to improve the oral bioavailability in presence and absence of lymphatic uptake compared with the free drug.

Materials and methods

Materials

Ibrutinib and sorafenib were obtained from MSN Laboratories Pvt. Ltd. Hyderabad, India. D-α-Tocopherol polyethylene glycol 1000 succinate (TPGS), poloxamer-188 (Pluronic® F-68) and poloxamer-407 (Pluronic® F-127) were obtained from Sigma-Aldrich, India. Sodium lauryl sulphate (SLS), hydroxy propyl methylcellulose (HPMC E-15), povidone K-30 (PVP K-30), trifluoroacetic acid, acetone and mannitol were purchased from SR life sciences, India. Polysorbate (Tween®80) was from SD fine chemicals, India. Glycerol monostearate (GMS), palmitic acid, stearic acid, trimyristin, trilaurin and tripalmitin were obtained from Alpha Aesar, India. Compritol ATO 888®, Capryol™ PGMC, Labrafil® (LBF), Labrasol® (LBSL), Lauroglycol® (LGL) and Capmul MCM8® were obtained as gift samples from Gattefosse, saint-priest Cedex, France. Isopropyl myristate (IPM), oleic acid and tristearin were purchased from TCI Chemicals Pvt. Ltd. India.

Reverse phase high-performance liquid chromatography

Chromatographic estimation of IBR was achieved using the method with Inert sustain® C18 column (150 × 4.6 mm, 5 μm) connected to reverse phase high-performance liquid chromatography (RP-HPLC) (Shimadzu, Cort, Japan) equipped with degasser (DGU-20A), pump (LC-20 AD), auto-injector (SIL-20 AC HT fixed with a 100 μL loop), oven (CTO-10AS VP) and UV-Visible detector (SPD-20A). The developed method consisted of water (A) (pH 5.0 adjusted with dilute trifluoroacetic acid) and acetonitrile (B) as mobile phase. Gradient elution was performed where the % B was varied at pre-determined time intervals; 40% of B was run until 1 min. Furthermore, it was increased to 90% (1.0 to 2.0 min) and continued from 2.0 to 4.0 min, after which a slow decrease to 40% was carried up to 6.0 min. Finally, 40% was continued from 6.0 to 10.0 min and the detection was performed at 258 nm [25].

Screening studies

Liquid lipid screening

Liquid lipid screening was based on the ability of the liquid lipid to solubilise IBR. Briefly, 1 mL of each lipid was taken into 2.0 mL micro centrifuge tube (Tarsons-500020). Excess IBR was added, vortexed and kept in a rotary orbital shaker (Lab companion SI-300) for 72 h at 37 °C. Samples were collected and subjected to centrifugation for 10 min at 15000 rpm; supernatants were filtered through 0.45 μm PVDF syringe filter. After filtration, measured quantity of methanol was passed through the filter to solubilise the drug if adsorbed to membrane. Later, the samples are suitably diluted and analysed by RP-HPLC [26].

Solid lipid screening

Various solid lipids were weighed accurately (500 mg) and added to 3 mL glass vial which was then heated to 5 °C above their melting point to ensure complete melting of the solid lipids. To these molten lipids, IBR was added in increments and visually checked for any un-dissolved drug [27].

Affinity/partition study

A saturated solution of IBR in Milli-Q water was prepared by addition of excess drug to 35 mL of water and the undissolved drug was removed by filtration using 0.22-μm membrane filter. Individual solid lipids (200 mg) were added to 5 mL saturated drug solution and heated to 75 °C. Samples were kept in a trembling water bath (Julabo, SW 22) maintained at 75 °C for 1 h. Later, the samples were left to attain room temperature and were then centrifuged at 10000 rpm for 10 min to separate the water and solid lipid. The solid lipid was dissolved in methylene chloride which was further diluted suitably. Both water and lipid phases were analysed using RP-HPLC to calculate the content of IBR and the drug entrapped in each solid lipid was calculated [28].

Screening solid-liquid lipid ratios

NLC are composed of solid and liquid lipids whose compatibility is indispensable to obtain the right formulation. Compatibility amongst the screened lipids was studied by mixing the solid and liquid lipids at various ratios (100:0, 90:10, 80:20, 70:30, 60:40, 50:50, 40:60 and 30:70). These lipids were mixed properly and filled into capillary tubes for the determination of melting point using melting point apparatus (Stuart SMP30) [28]. Furthermore, the lipid matrices were melted and transferred on to a watch glass and left for solidification at room temperature. Whatman® filter paper was gently pressed against each of the solid matrices to determine the oozing of the liquid lipid out of lipid matrix [29].

Surfactant screening

Selection of surfactant was done by one-factor at a time approach (O-FAT). Different formulations containing individual stabilisers at constant concentrations were prepared and the screening was done based on the size and PDI [15].

Preparation method

Briefly, weighed quantities of solid, liquid lipids and IBR were taken in an organic mixture (acetone and ethanol in 1:1 ratio). The aqueous surfactant solution was prepared by adding the surfactant to 10 mL of water and heated to 60 °C. Organic mixture was heated until the temperature reaches to 60 °C. The heated organic solution was added to hot surfactant solution under stirring at 500 rpm for 1 min. This mixture was sonicated at amplitude of 40 W, using a pulse of 10-s on and 5-s off (Sonics & Materials, Inc., Vibra cell VCX 750). Soon after the sonication, stirring was continued at 800 rpm for 4 h. Furthermore, the formulations were subjected to rotary vacuum evaporator at 40 °C under reduced pressure to ensure complete removal of solvent [27, 30, 31].

Design of experiments

Drug regulatory bodies like USFDA, TGA, MHRA and EMA do not encourage quality by testing rather they encourage the quality by design (QbD) [32]. QbD is a systematic approach for product development with pre-defined goals that involve prior knowledge, design of experiments (DoE), risk assessment and knowledge management throughout the product life cycle. QbD integrates the product quality at the time of development, unlike the traditional approach where the quality is tested post production [33]. It provides a better understanding of the interrelationships existing between each factor and effect of these factors onto the corresponding variables. QbD requires minimum number of runs thus decreasing the cost, time and efforts compared with conventional approach [34, 35]. QbD approach comprises of establishing the quality targeted product profile (QTPP), identifying the critical quality attributes (CQAs), critical material attributes (CMAs) and critical process parameters (CPPs). In this study, QbD was applied in the following steps:

i. An initial risk assessment by cause and effect relationship to identify the variables affecting the CQAs.
ii. Screening of factors by Plackett-Burman design (PBD).
iii. Optimisation and embarking design space by means of response surface methodology (RSM) (central composite design (CCD).

iv. Checkpoint analysis for the validation of the developed design.

QTPP and CQAs

QTPP comprises of prospective summary of desired characteristics of the final product that ensure the quality, safety and efficacy of the product. Defining QTPP is the primary step in QbD; it is also considered "goal or objective setting" step followed by, identification of CQAs, which are product-centric properties or characteristics whose control within the limit ensures the product quality [36, 37].

Risk assessment and identification of critical material attributes and critical process parameters

Risk assessment step deals with listing of various factors that may affect the final parameters (CQAs). Furthermore, amongst various factors listed the factors with high impact over the CQAs are to be identified. Raw material (formulation)–related factors affecting CQAs are termed as critical material attributes (CMAs) whereas the process-related factors are called critical process parameters (CPPs) [38].

Screening of significant factors using Plackett-Burman design

To estimate the significance of various factors on the responses, screening with Plackett-Burman design (PBD) was performed. PBDs are two-level fractional factorial screening designs suitable when a large number of factors are involved. Based on the preliminary studies, it was observed that formulations with solid lipid content of 50 to 250 mg were stable and uniform. However, factors like liquid lipid and drug content are dependent on solid lipid content. In order to avoid any change in the solid lipid content, further studies were performed with 200 mg of solid lipid. The six variables screened by PBD are shown in Table 1 with their upper and lower limits. Effects of these variables on the IBR-NLC characteristics (responses Y1: particle size, Y2: polydispersity index (PDI) and Y3: entrapment efficiency Screening of significant factors using Plackett-Burman design (E.E.)) were screened. A total of 12 experimental runs (3 centre point replicates) were generated by the Design-Expert® 11.0 software (Stat-Ease Inc., Minneapolis, MN, USA).

Table 1 Levels of each variable for PBD

	Variables	Lower level	Upper level
A.	Liquid lipid (% of solid lipid)	10	50
B.	Drug (% of lipid)	5	15
C.	Surfactant (%*w*/*v*)	0.25	2.00
D.	Organic to aqueous ratio	0.2	0.6
E.	Stirring speed (rpm)	400	1200
F.	Sonication (time in min)	5	15
	Responses	Constraints	
Y_1	Particle size	Minimise	
Y_2	PDI	Minimise	
Y_3	E.E.	Maximise	

Central composite design

The factors which are proven to be significant (from PBD) are further analysed by response surface design i.e. central composite design (CCD). CCDs are full factorial designs in which each factor has five levels: $-\alpha$ (axial point), low level (− 1), one centre point (0), high level (+ 1) and $+\alpha$ (axial point) [39]. The responses (dependent variables) remained the same as in the case of PBD. A total of 19 runs were suggested by the software.

Search for optimised formulation and design space Search for the best formulation was done by numerical optimisation using the desirability function. The targeted values for each response are provided for which various solutions with a specific desirability value are obtained ranging from 0 to 1. The higher the value, the more is the assurance of obtaining the desired results; the optimum formulation is the one which has the highest desirability value. Graphical optimisation was performed by design space [40].

Validation of the design The design utilised was further validated by checkpoint analysis. Three confirmatory trials were performed at and the results obtained were compared with the predicted values [33].

Multivariate analysis

Additionally, a distinctive way of validating the design output was carried out by various multivariate data analysis tools which include principal coordinate analysis (PCoA), bubble plot and normal probability plot. The plots generated were then interpreted and cross verified with the DoE results [37, 41, 42].

Characterisation

Particle size, polydispersity index and zeta potential

Formulations were diluted approximately 10 folds with Milli-Q water and analysed by Malvern Zetasizer Nano ZS (Malvern Instrument Ltd., Worcestershire, UK). Particle size and PDI measurement are based on the principles of dynamic light scattering, and the Stokes-Einstein relation was applied for the conversion of measured Brownian motion of particles into size and size distribution [39, 43].

Entrapment efficiency

In brief, 1 mL of the formulation was centrifuged using ultracentrifuge (Thermo scientific Sorvall MX 150 Plus) at 1,00,000 rpm for 60 min at 4 °C. The supernatant was collected and the amount of free drug (W_{free}) was analysed at 258 nm using HPLC [44].

$$EE\ (\%) = \frac{W_T - W_{Free}}{W_T} \times 100$$

W_T total drug added.
W_{free} free drug.

Morphology

Surface morphology of the developed NLC and free drug was studied using field emission scanning electron microscope (FESEM) (Quanta 400 SEM; FEI Company, Cambridge, UK). Samples were positioned on SEM specimen stubs using two-sided carbon adhesive tape. These stubs were sputter-coated with gold for 5 min and analysed (FEI Tecnai G2F20, Netherlands) at an accelerating voltage of 200 kV [10, 39]. Surface morphology was further studied using transmission electron microscopy (TEM). The samples were diluted (100 ×) using Milli-Q water and placed on to a film-coated copper grid and negatively stained with 1% *w*/*v* uranyl acetate and allowed to dry. Excess liquid was drained off and the grid containing the nanoparticle sample as a dry film was observed with a transmission electron microscope JEM 2100 (JOEL, Tokyo, Japan) with an accelerating voltage of 120.0 kV using Digital Micrograph® software (Gatan, Inc., San Francisco, CA, USA) [44].

Lyophilisation

The optimised formulation was lyophilised (Lyophilizer Lab India FD5508) for enhancing the stability and ease of handling. Formulation to be lyophilised was filled into round cryochill flasks with 1% *w*/*v* mannitol as cryoprotectant. Primary freezing of the samples was achieved using dry ice at atmospheric pressure; later, the samples were connected to the lyophiliser for secondary drying. The initial freezing was performed at − 60 °C. Furthermore, the condensation was carried out at − 80 °C under 150 mTorr pressure. The primary drying was done at 20 °C for 2 h, under 150 mTorr of pressure. A secondary drying phase was performed at 25 °C, for 4 h, under 100 mTorr of pressure [15].

Attenuated total reflectance Fourier transform infrared spectroscopy

Presence of any possible drug-stabiliser interactions was elucidated by Shimadzu 8400 spectrophotometer. Samples were scanned at wave numbers ranging between 400 and 4000 cm^{-1} with a resolution of 1.0 cm^{-1}. Free drug, GMS, Pluronic® F-127, physical mixture (IBR + GMS + Capryol™ PGMC + Pluronic® F-127) and NLC were analysed to detect the presence of any interactions.

Thermal analysis

Thermal analysis of the samples viz. free drug, GMS, Pluronic® F-127, physical mixture (IBR + GMS + Capryol™ PGMC® + Pluronic® F-127) and NLC formulations were carried out by differential scanning calorimeter (DSC) (Mettler Toledo DSC-1). Approximately, 1–2 mg of sample was kept in aluminium pans and heated from 25 to 200 °C at a rate of 10 °C/min [40].

Powder X-ray diffraction

To study the polymorphic nature of the formulations, powder X-ray diffraction (PXRD) was performed in reflection mode using Cu-Kα radiation generated at 40 kV and 40 mA (D8 Advance, Bruker, Germany). The X-ray diffractograms generated were then compared with free drug to check for polymorphic transformations occurred during formulation process [26].

In vitro drug release

In vitro release study of the optimised NLC formulation and free IBR suspension was performed using dialysis bag made by dialysis membrane (MWCO 12000, Hi Media). The membrane was activated as per the procedure provided by the manufacturer. Formulation equivalent to 2 mg of IBR was filled in the bag and placed in 50 mL phosphate buffer (pH 6.8) maintained at 37 °C and stirred at 100 rpm [7]. Aliquots of 5 mL were collected at pre-determined time points and fresh media was added to maintain the sink condition. The samples were further analysed using HPLC and the data was subjected to various kinetic equations to investigate the mechanism of drug release [8].

Stability study

The optimised formulation was subjected to stability studies at 4 °C and 25 °C at 65% RH for 1 month. At each predetermined time interval (10, 20 and 30 days), the samples were taken and measured for particle size, PDI and E.E.

Pharmacokinetics

Sample extraction and bioanalysis

Extraction of IBR from plasma samples was achieved by protein precipitation. Briefly, 250 μL of acetonitrile with internal standard (Sorafenib) was added to 50 μL rat plasma and vortex mixed, centrifuged at 10000 rpm for 10 min. The supernatant was collected and analysed by the above described RP-HPLC method (section 2.2). The peaks of IBR and IS were well separated with retention times 7.10 min and 8.01 min respectively, and the resolution was 6.08. Sorafenib and ibrutinib are > 99% base and produces linear results, in selected method and UV absorption conditions. If the study needed to be done at very low concentrations, sorafenib offers very high sensitivity towards detection. The method was further validated for the parameters such as specificity, linearity/range, sensitivity, accuracy, precision, recovery and robustness [45].

Animal studies

All the animal experiments were conducted in accord with the guidelines of the committee for the purpose of control and supervision of experiments on animals (CPCSEA), Government of India. Experimentation was performed as per animal protocol (NIP/01/2018/PE/262) approved by Institutional Animal Ethics Committee (IAEC) NIPER, Hyderabad. Male Wistar rats, weighing about 225.45 ± 11.9 g, were housed under the environment of controlled temperature (22–26 °C) and light (12 h light/dark cycle) with free access to water. Animals were segregated into two groups (A and B) containing six rats each. Group A was administered with free IBR (dispersed in 0.5% *w/v* sodium carboxymethyl cellulose and group B was administered with NLC formulation.

Both the groups received oral dosing equivalent to 12.5 mg of IBR per kg of rat [7], and at pre-determined time intervals, the rats were anaesthetised with isoflurane and around 300 μL of blood samples were withdrawn from retro-orbital plexus into Eppendorf tubes containing EDTA. Plasma was obtained by centrifugation at 10000 rpm for 10 min. The samples were processed and analysed by RP-HPLC method [40].

Lymphatic uptake study by chylomicron flow blocking approach Chylomicron flow blocking approach using cycloheximide (CXI) was utilised to evaluate the ability of the developed formulations to undergo lymphatic uptake. CXI is a protein synthesis inhibitor that blocks the production of chylomicrons and thus obstructs the lymphatic transport. Hence, administration of free drug and formulation in the presence of CXI will not have lymphatic uptake. On the other hand, in the absence of CXI (i.e. in groups A and B), there is no obstruction in the lymph production; hence, the free drug or formulation may enter into lymph based on their ability to do so.

The animals were divided into two groups (C and D) with six animals each. Animals received 3.0 mg/kg of intraperitoneal CXI. After 1 h of CXI dosing, the groups C and D were administered with free drug and optimised NLC (IBR equivalent to 12.5 mg/kg per rat) respectively. Blood sampling, processing and analysis were performed as discussed in section 2.11.1 [8, 46, 47].

Data analysis

The concentration-time profile obtained was subjected to data analysis by WinNonlin (version 3.1; Pharsight Co., Mountain View, CA, USA). The non-compartmental analysis was used to estimate the pharmacokinetic parameters. The pharmacokinetic parameters were expressed as mean ± standard deviation (SD). The parameters were further subjected to statistical analysis using the Graph Pad Prism software (Graph Pad Software Inc., San Diego, CA).

Results and discussion

Screening of solid and liquid lipids

Higher drug loading and entrapment are the prime requirements for the formulation, which can be achieved by the selection of lipids with higher drug solubility. Hence, screening of lipids was done based on the solubility of the drug [48]. As represented in Fig. 1, amongst various liquid lipids screened, Capryol™ PGMC has shown the highest IBR solubility (55.24 ± 3.54 mg/mL). Furthermore, IBR solubility and affinity were tested in glycerol monostearate, stearic acid, tripalmitin, tristearin, trilaurin, palmitic acid and compritol ATO 888®. IBR had the highest solubility in GMS (as seen by visible method). As shown in the supplementary Fig. 2, GMS was found to have the highest entrapment/affinity of IBR compared with the other solid lipids; hence, GMS was selected as solid lipid.

Screening solid-liquid lipid ratio

GMS in the absence of liquid lipid showed a melting at 63.3 °C. Addition of liquid lipid to solid lipid resulted in the decrease of melting point indicative of miscibility of solid and liquid lipids (Fig. 2). Furthermore, lipid mixtures when analysed by Whatman® filter papers, no liquid lipid oozing out was noticed up to 50%. A proper solid and liquid lipid ratio is important not only to hold the drug inside the carrier but also to maintain the consistency at room temperature.

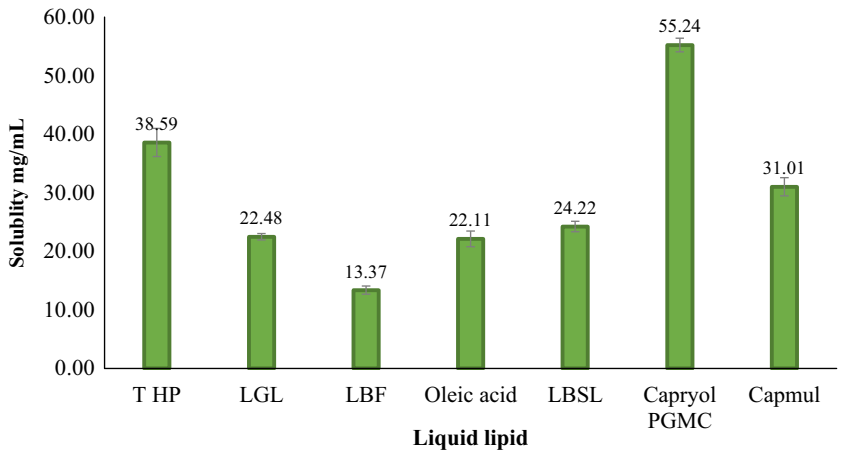

Fig. 1 Solubility of IBR in various liquid lipids ($n = 3$, data presented as mean ± SD) (*THP*, Transcutol® HP, *LGL* Lauroglycol, *LBF* Labrafil, *LBSL* Labrasol)

Hence, based on these studies, the maximum lipid percentage was fixed at 50%.

Screening of surfactant

Screening of stabiliser was done by preparing various formulations with the selected GMS and Capryol™ PGMC as solid and liquid lipids, by using 1% *w/v* each of individual stabilisers like TPGS, Tween®80, cremophor RH40® and Pluronic® F-127. The results are shown in supplementary Table 1. Amongst all the surfactants, Pluronic® F-127 resulted in the lowest particle size (109.52 ± 4.21 nm) and PDI (0.180 ± 0.022). Hence, Pluronic® F-127 was selected as stabiliser for further studies.

Design of experiment

QTPP and CQAs

The target of the study was to develop NLC as a carrier system aimed at lymphatic uptake thus enhancing the oral bioavailability of IBR. Identifying the CQAs is the preliminary step in the QbD approach and control of CQAs within limit ensures the achievement of QTPP. As shown in Table 2, particle size, PDI and E.E. were selected as CQAs. Size affects the uptake phenomenon, smaller the particles size easier is the penetration. Also, size reduction confers the availability of the drug in dispersed form thus enhancing the dissolution. PDI is a dimensionless parameter which provides an idea about the distribution of particles in the system, whether they are mono or hetero-disperse. The particle size and PDI help in checking the stability of the formulation (aggregation can be seen in unstable formulations) [36]. E.E. is the amount of drug that is incorporated into the nanoparticles. Increase in E.E. is desired to have the advantages rendered by the formulation [37].

Risk assessment and identification of CMAs and CPPs

Initial risk assessment was performed by creating an Ishikawa (fish-bone) diagram (Fig. 3) which shows the cause and effect relationship (effect of each variable on the CQAs). Amongst the listed factors, only the significant factors (formulation and process) were further considered for screening trials [49].

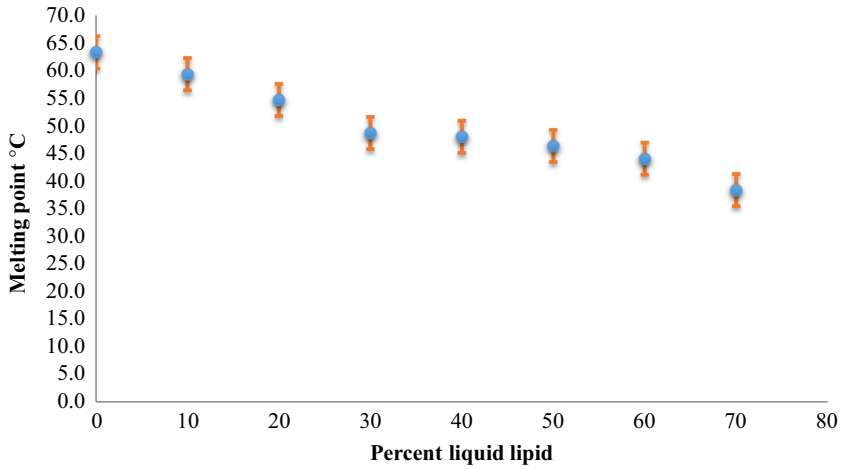

Fig. 2 Graphical representation of change in melting point with addition of liquid lipid i.e. Capryol™ PGMC ($n = 3$, data presented as mean ± SD)

Table 2 QTPP and CQA identification

QTPP	Target	Justification
Formulation	Nanostructured lipid carriers	NLC formulation can enhance the lymphatic uptake and reduce the first pass metabolism of the drug thereby, increases the bioavailability
Route of administration	Oral	Marketed formulation is oral, and the target is to enhance the oral bioavailability
Pharmacokinetics	Should be better than already available form	For increased bioavailability
Stability	No visible signs of aggregation/cake formation up to 20 days after formulation	The efficiency of the formulation depends on particle size, and hence, it is important to maintain the same
CQAs		
CQA	Target	Justification
Particle size	Mean particle size below 200 nm	Size reduction to nano-scale increases surface area which in turn increases the solubility and dissolution. Increased solubility and dissolution result in increased bioavailability and reduction in food-related pharmacokinetic variation
PDI	Less than 0.5	PDI greater than 0.5 indicate broader distribution (hetero-disperse). Moreover, such formulations are not suitable for particle size measurement by DLS
Entrapment efficiency (E.E.)	Higher	Higher EE ensure higher drug loading in the carrier system

Screening by Plackett-Burman design

Prior to optimisation design, identifying the most significant factors affecting CQAs is necessary. PBDs are resolution III designs that screen the factors at two levels to provide the significance of each factor in an economical way. Since PBD analyses the significance of each factor with a minimum number of runs, the results are often perplexed; hence, these designs are used for screening purpose only. In this study, a two-level six-factor PBD was applied to study the significance of each factor. As shown in the Pareto charts (Fig. 4), the liquid lipid amount, drug amount and surfactant concentration were found to be the significant factors. Hence, the abovementioned factors were selected for further optimisation trials. Based on the results, the non-significant factors were fixed as solid lipid 200 mg, aqueous volume 10 mL, organic solvent 4 mL (2 mL each of ethanol and acetone), sonication time 10 min and a stirring speed of 800 rpm.

Central composite design

The factors along with their limits for further screening with CCD are shown in Table 3. The results obtained after performing the trials were subjected to multiple linear regression for the generation of polynomial models like linear, quadratic and two-factor interaction (2FI). Model selection was done based on the predicted R^2, adjusted R^2 and coefficient of variation (CV). Furthermore, the importance of variables on the responses was analysed by ANOVA.

Particle size The particle size of the obtained formulations was in the range of 98.74 to 551.04 nm. Design suggested the 'quadratic' model which was found to be significant and the lack of fit was insignificant. The model F value obtained was 919.01 which imply there is 0.01% chance it may be due to noise. ANOVA was performed to identify the significance of each variable on the response. Independent variables with a p value < 0.05 are considered to be significant. The R^2, adjusted R^2 and predicted R^2 values were 0.98, 0.97 and 0.90. The adequate precision obtained was 25.24 which is more than the required value of 4, indicating high signal to noise ratio and the model being capable of exploring the design space [50]. The p values of the model term A, B, C, AB, BC, A^2 B^2 and C^2 were found to be < 0.05 indicating their significant role in the response. Hence, these terms are considered significant and the resultant regression equation was

$$\text{Particle size} = 102.89 + 37.91A + 49.75B + 18.82C - 22.44\text{AB} - 0.52\text{AC} + 25.87\text{BC} + 69.05A^2 + 84.42B^2 + 54.33C^2$$

The effect of each variable on the particle size is depicted by perturbation plots of Fig. 5a. Furthermore, the significance of each factor can be explained by 3D response surface plots (supplementary Fig. 3) and by the equation provided above. As seen in the equation, the particle size is affected by the factor B i.e. the drug added. This can be due to an increased drug loading causing an increase in interfacial tension thus decreasing the efficiency of the surfactant in reducing the particle size. Increase in liquid lipid (factor A) decreased the particle size up to certain extent after which the particle size increased. Increase in particle size with liquid lipid can be supported by increased E.E. with increased liquid lipid. Moreover, in core-shell type NLC, the liquid lipid is present as a core surrounded by solid lipid in such cases particle size is

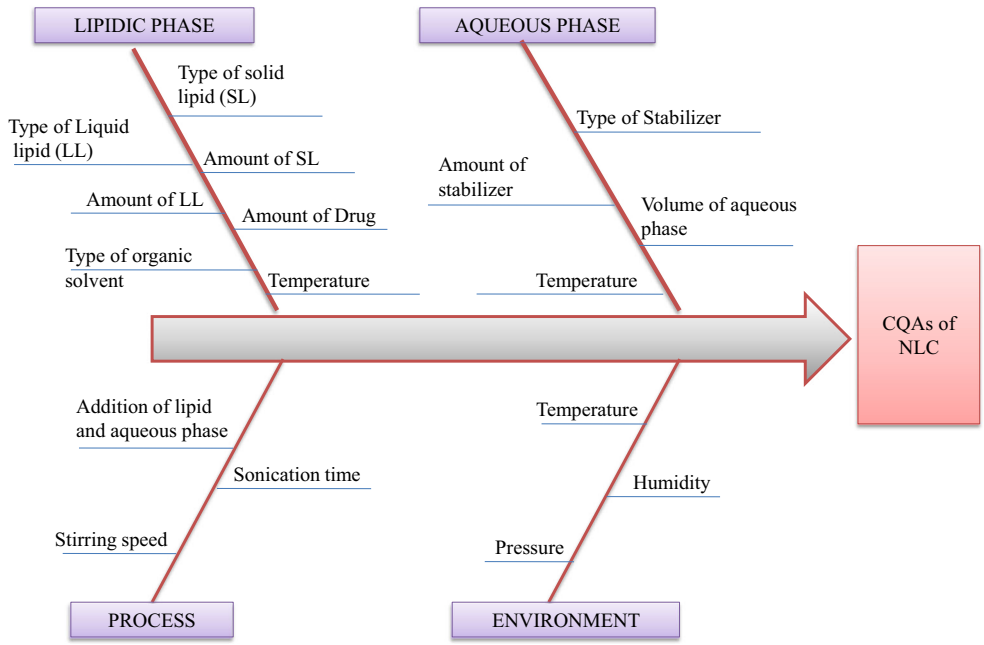

Fig. 3 Ishikawa (fish-bone) diagram showing cause effect relationship for the production of NLC

increased with increased lipid content. At lower amount, the stabiliser may not be sufficient to prevent the increase in particle size, and at higher amounts, the particles may be coated with stabiliser and resulting in increased particle size. The effect of various factors on the particle size was in harmony with the previous reports [20, 26, 40, 49, 51].

PDI It is a dimensionless parameter which is the measure of the distribution of particles (broadness of size). It ranges from 0 to 1; however, if the value is > 0.5, the sample has a broad distribution of particles (hetero-disperse) which is indicative of instability (non-uniformity). Hence, such formulations are not desired [52]. The PDI was in the range of 0.146 to 0.872. Design suggested the 'quadratic' model which was found to be significant and the lack of fit was insignificant. The model F value obtained was 30.14 which imply there is a 0.1% chance and it may be due to noise. ANOVA was performed to identify the significance of each variable on the response, independent variables with p value < 0.05 are considered to be posing significant effect over the response and non-significant variables are removed for model improvement. The R^2, adjusted R^2 and predicted R^2 values were 0.96, 0.93 and 0.82 respectively. The adequate precision value was 20.78 which is more than the required value of 4, indicating the model can be used to explore the design space. The p values of the model term A, B, AC, BC, A^2 and B^2 were found to be < 0.050 indicating their significant role in the response. Hence, these terms are considered significant and the resultant regression equation was

$$\mathrm{PDI} = 0.306 + 0.103A + 0.157B + 0.054\mathrm{AC} + 0.068\mathrm{BC} + 0.097A^2 + 0.053B^2$$

As shown in the perturbation plots (Fig. 5b) and response surface plots (supplementary Fig. 4), an increase in the liquid lipid and drug increased the PDI. As discussed above, an increase in lipid and drug might have caused an increase in loading thus resulting larger particles, resulting in variation in particle size [26, 53].

Entrapment efficiency Entrapment efficiency provides an idea about the amount of the drug that is incorporated into nanoparticles. The entrapment efficiency (E.E.) of the developed formulations was in the range of 36.78 to 87.40. Design suggested the 'quadratic' model which was found to be significant and the lack of fit was insignificant. The model F value obtained was 18.93 which imply there is 0.01% chance it may be due to noise. ANOVA was performed to identify the significance of each variable on the response; independent variables with p value < 0.05 are considered to be significant. The R^2, adjusted R^2 and predicted R^2 values were 0.94, 0.89 and 0.72 respectively. The adequate precision obtained was 14.82 which is more than the required value of 4, indicating the model is capable of exploring the design space [50]. The p-values of the model term A, C, AB, AC, BC, A^2, B^2 and C^2 were found to be less than 0.05 indicating their significant role on the response. Hence, these terms are considered significant and the resultant regression equation was

$$E.E = 71.83 + 10.00A + 5.84C - 3.74\mathrm{AB} - 5.82\mathrm{AC} - 4.28\mathrm{BC} - 5.18A^2 + 4.81B^2 - 4.50C^2$$

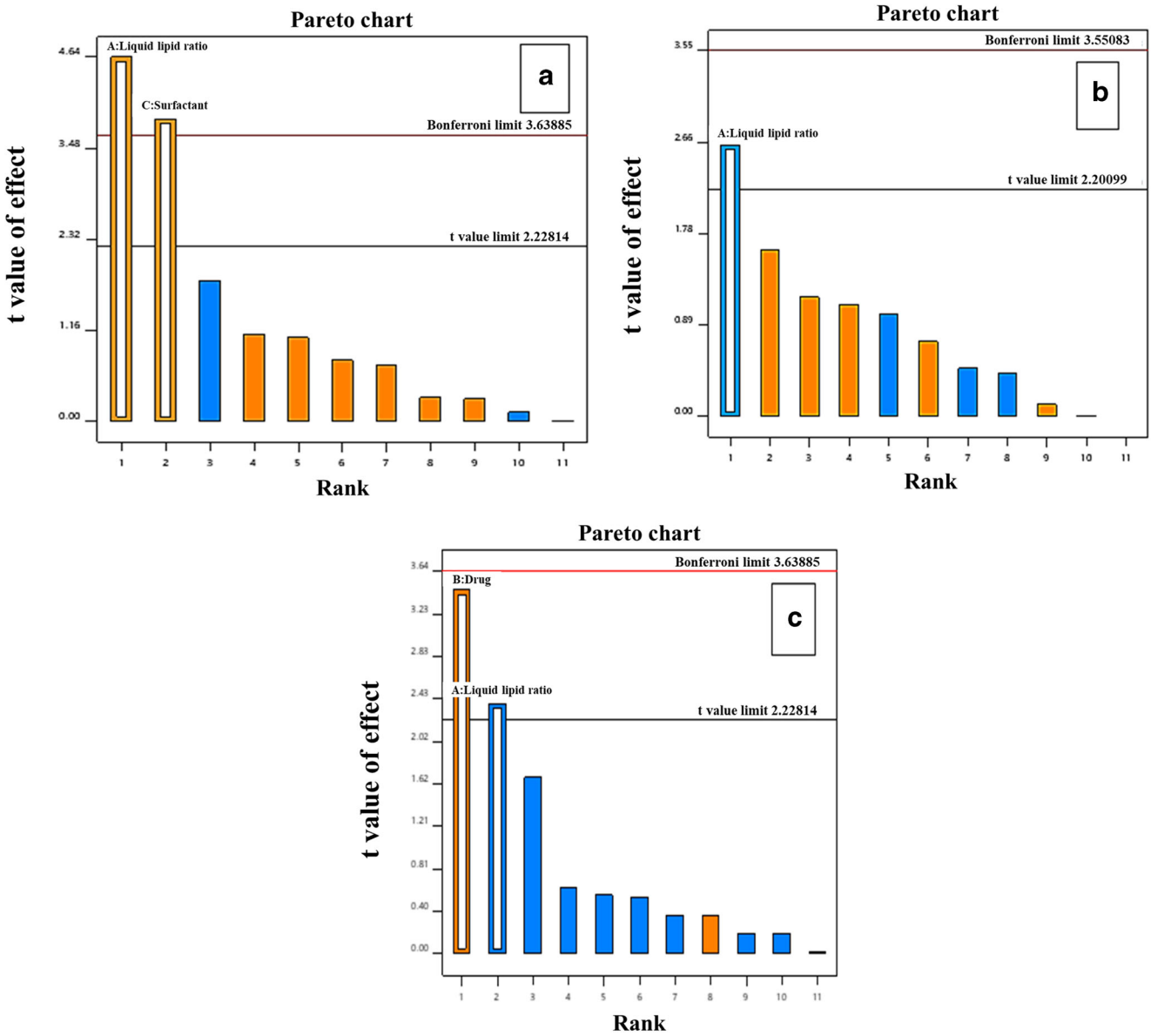

Fig. 4 Pareto charts displaying the significance of each factor: **a** particle size **b** PDI and **c** E.E.

The factors *A* (liquid lipid) had a significant impact on the response E.E. As shown in the supplementary Fig. 5 and perturbation plot (Fig. 5c), the liquid lipid content and surfactant concentration had a direct relationship with the E.E. Since the drug has more solubility in the selected lipids, an increase in liquid lipid increases the solubilisation of the drug thus leading to the incorporation of more amount of drug. Increase in the surfactant concentration increased the E.E. to certain extent, after which a reduction in E.E. was noticed. Excess surfactant might have solubilised the drug leading to reduced E.E. The effects of various independent parameters on E.E. were in agreement with the previously published results [20, 49, 53, 54].

Table 3 Factors and levels used in CCD

Factor	Name	Units	Type	− α	+ α	− 1	+ 1	0
A	Liquid lipid		Numeric	0.0977	0.6023	− 1 ↔ 0.20	+ 1 ↔ 0.50	0.3500
B	Drug	% of total lipid	Numeric	1.59	18.41	− 1 ↔ 5.00	+ 1 ↔ 15.00	10.00
C	Surfactant	% *w/v*	Numeric	0.3239	2.43	− 1↔ 0.75	+ 1 ↔ 2.00	1.37

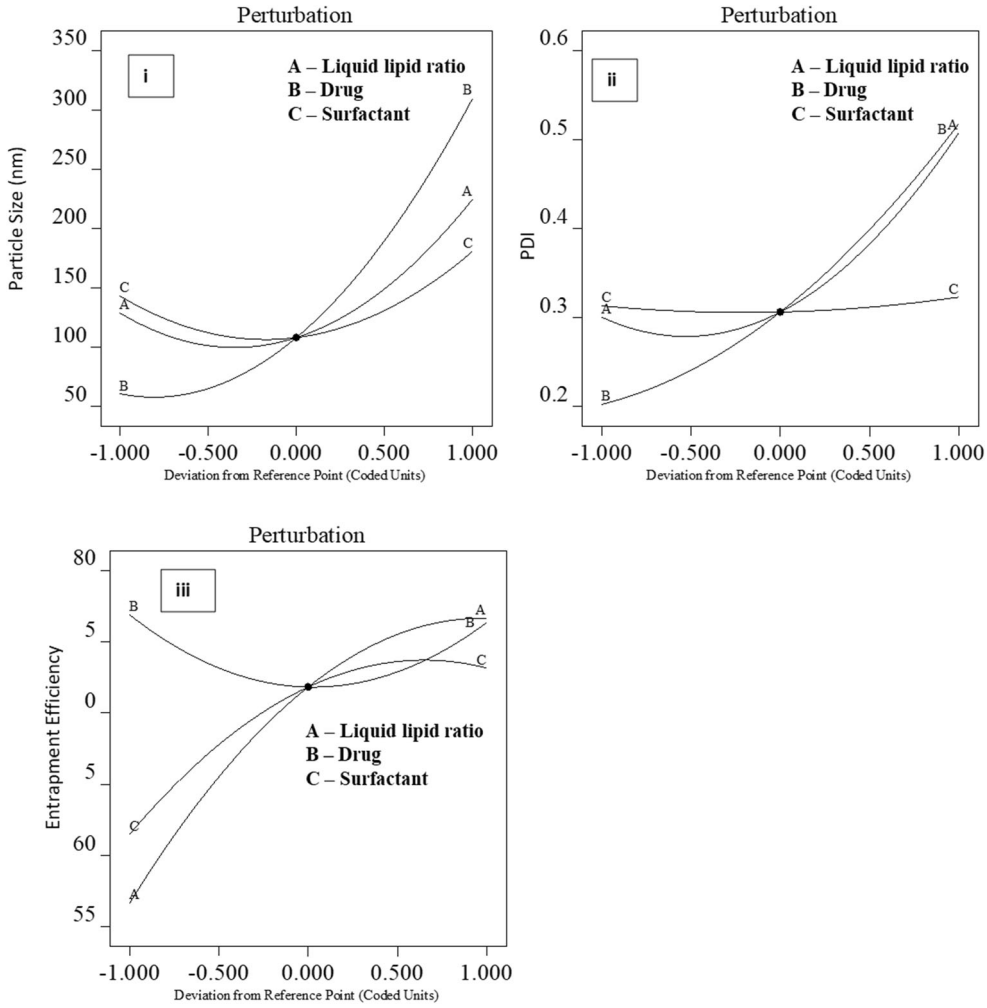

Fig. 5 Perturbation plots showing the effect of variables A—liquid lipid, B—drug and C—surfactant on the (i) particle size; (ii) PDI and (iii) E.E

Search for optimum formulation and design space After studying the effect of each independent factor on the response, search for the optimal formulation was done by numerical and graphical methods. In both the methods, the targeted values for each CQA shall be provided. In numerical optimisation, the design provides a list of solutions for the desired output; each of these solutions has a value from 0 to 1. As discussed above, the desirability value of 1 is the highest level of desirability. In this study, the desirability of 0.87 was obtained. The optimised formulation consists of 200 mg of solid lipid, 10 mL of aqueous volume, 4 mL of organic solvent (2 mL each of ethanol and acetone), 0.339% of liquid lipid, 10% of drug (% w.r.t total lipid) and 1.421% *w*/*v* of surfactant. Furthermore, graphical optimisation was performed to generate the design space. As shown in supplementary Fig. 6, a design space was obtained which has two regions yellow and grey areas representing the feasible and non-feasible areas respectively.

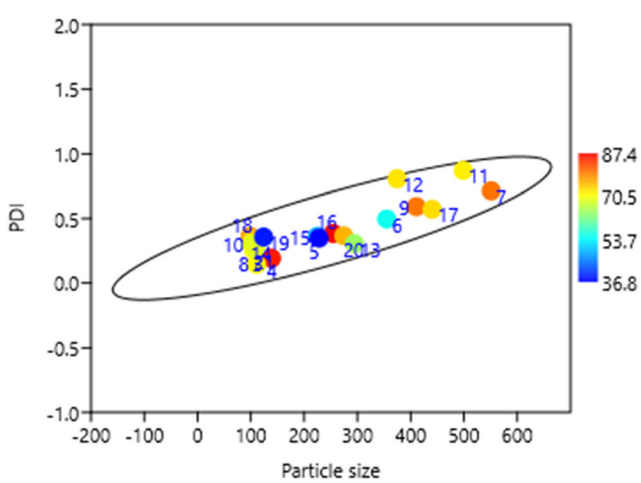

Fig. 6 Bubble plot describing the distribution of batches with respect to particle size, PDI and E.E. lying within the 95% confidence interval with no outliers present

Validation of the design

To establish the accuracy and robustness of the model, validation by three formulations was selected as checkpoints at various levels and prepared. The predicted mean values for size, PDI and E.E. were as 104.08 nm, 0.306 and 71.83%

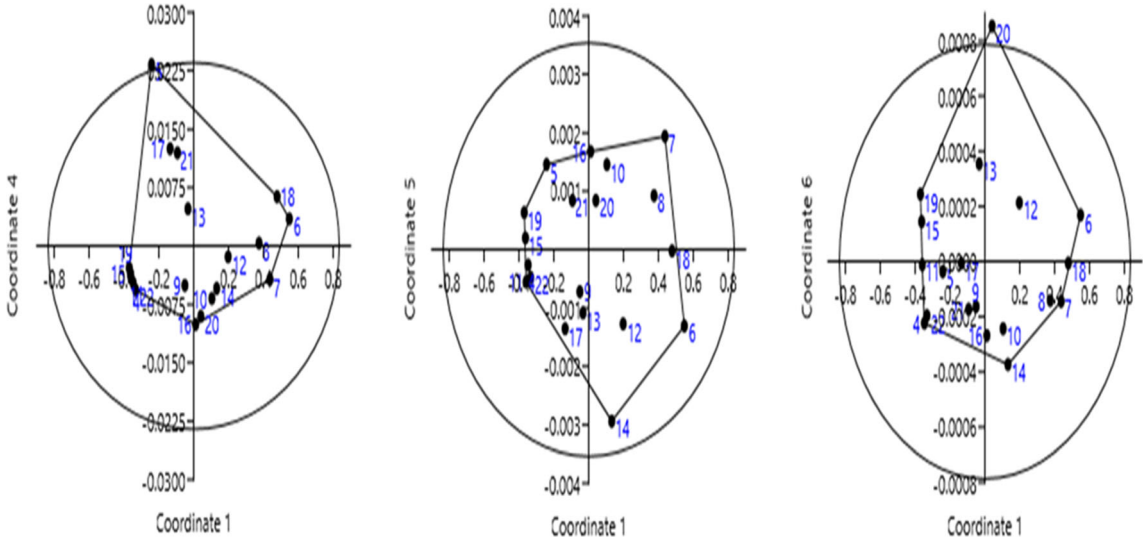

Fig. 7 Principal co-ordinate analysis plots for particle size, PDI and E.E. indicating the batches within the confidence interval range as a part of design suitability and validation

respectively, whereas the observed mean values of size, PDI and E.E. were 106.63 ± 8.66 nm, 0.283 ± 0.005 and 74.32 ± 5.52% respectively. The results obtained by these formulations were within the 95% confidence intervals provided by the software, thus validating the model developed.

Multivariate analysis

Normal probability plot

As shown in the supplementary Fig. 7, the plot signifies the importance and impact of the factors chosen: liquid lipid (A), drug (B) and surfactant concentration (C) over the responses selected from the screening design implying D as particle size, E as PDI and F as E.E. Such a high value of correlation coefficient implicates a strong interrelationship between the factors and variables and that a good correlation is obtained between them.

Bubble plot

Bubble plot enables to visualise responses in a 3D view, where every batch with their responses will be depicted graphically. As depicted in Fig. 6, the plot has particle size, PDI and Screening of significant factors using Plackett-Burman design E.E. as the X, Y and Z axis. The response of each batch is depicted and transition in colour of the bubble from blue to red implicates increase in entrapment efficiency of each batch. The 95% elliptical boundary represents the confidence of the design and suggests that all the batches are within the ellipse boundary are practically reproducible and that the data adequately fits the design [49].

Principle co-ordinate analysis

As shown in Fig. 7, it is evident that 93% of variance is due to axis 1 (i.e. liquid lipid content) which has significant importance and statistical dominance over all other factors. It

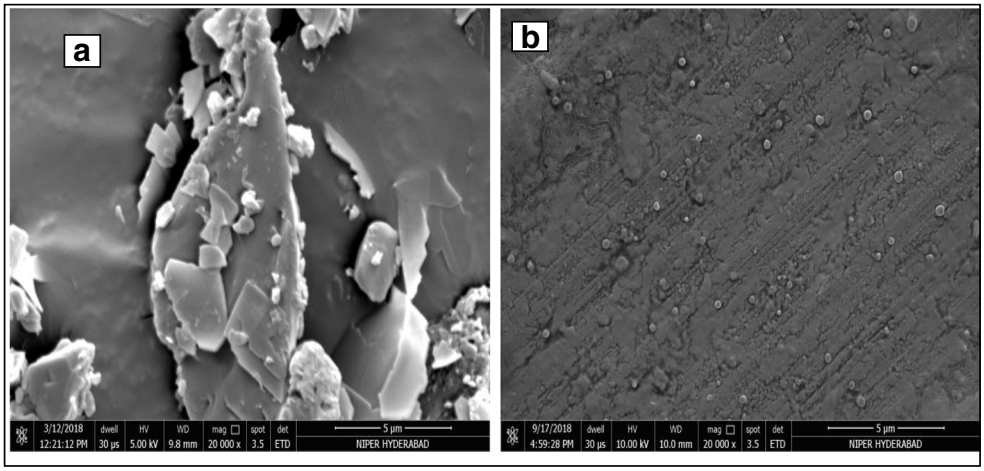

Fig. 8 Field emission scanning electron microscope (FESEM) images of (**a**) free drug and (**b**) NLC

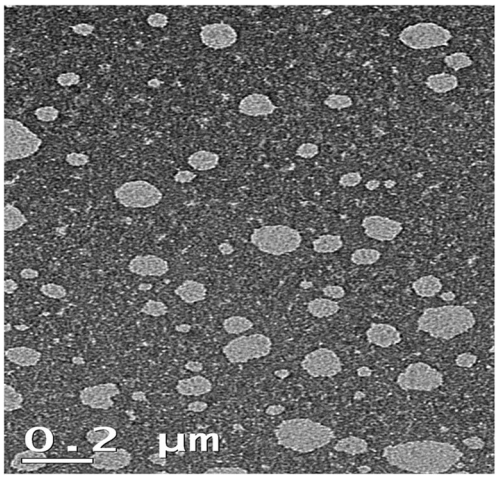

Fig. 9 Transmission electron microscopy (TEM) image of IBR-loaded NLC

suggests that the effect of liquid lipid content impacts all the responses. Batches are plotted by keeping liquid lipid content (coordinate 1) on the X-axis and the responses (particle size, PDI and entrapment efficiency) on the Y-axis (coordinate 4, 5 and 6 respectively). Highlighted hulls represent the distribution of batches. The circular area represents the 95% confidence interval within the data which is plotted. It is found that no outliers were found when the particle size and PDI were plotted against liquid lipid content; however, batch 20 was an outlier when entrapment efficiency was plotted against liquid lipid content. This implies that the design selected was appropriate and suitable for distinguishing between different variables and identifying the outliers and how it helped to create a suitable design space.

Characterisation

Morphology

Morphology of the free drug (A) and NLC (B) was studied using FESEM; the result is depicted in Fig. 8. The free drug was crystalline with discrete units scattered, whereas the NLC formed were spherical. As shown in Fig. 9, TEM analysis revealed spherical and mono-disperse particles.

Attenuated total reflectance Fourier transform infrared spectroscopy

Presence of any possible interactions free drug (ibrutinib), Pluronic® F-127, GMS, physical mixture and freeze dried NLC was scanned in the range of 4000–400 cm^{-1} using attenuated total reflectance Fourier transform infrared spectroscopy (ATR-FTIR) (Perkin Elmer). As shown in Fig. 10, free drug had characteristic peaks at 1652, 1613, 1520, 1241, 1147, 1100, 986 and 953 cm^{-1} [16]. Pluronic® F-127 shows peaks at 2882, 1374, 1360, 1343, 1281, 1242, 1149, 1113, 1060, 1012, 963 and 947 cm^{-1} [55]. GMS shows characteristic peaks at 2918, 2850, 1734.8, 1557.5, 1468.1, 1390.3, 1179.6, 1050 and 724.6 cm^{-1} [56]. The spectra obtained with physical mixtures are similar to the NLC formulations indicating the presence of IBR in the formulations. Additionally, it implies the absence of any chemical interaction between drug and other components.

Thermal analysis

DSC analysis was performed for free drug, Pluronic® F-127, GMS, physical mixture (drug + GMS + Capryol™ PGMC) and optimised NLC formulation. As shown in the thermograms (Fig. 11) free drug shows a sharp melting peak at 158 °C indicating the crystalline nature of the drug. GMS shows a sharp endothermic peak at 62.89 °C. DSC curves of NLC had two melting peaks which can be related to the presence of Pluronic® F-127 and GMS; surprisingly, there was no peak pertaining to IBR which suggests the formation of a molecular dispersion of drug into the melted lipid matrix. This can be further explained by Kelvin effect which states

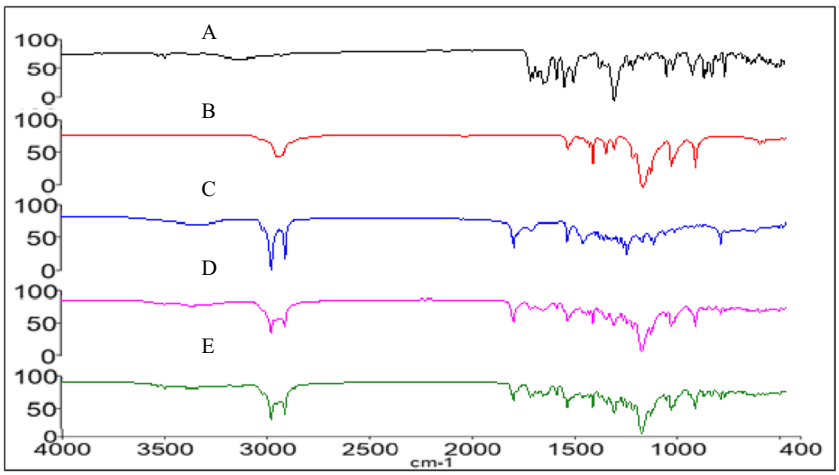

Fig. 10 ATR-FTIR spectra of A—free drug, B—Pluronic®F127, C—GMS, D—physical mixture and E—NLC

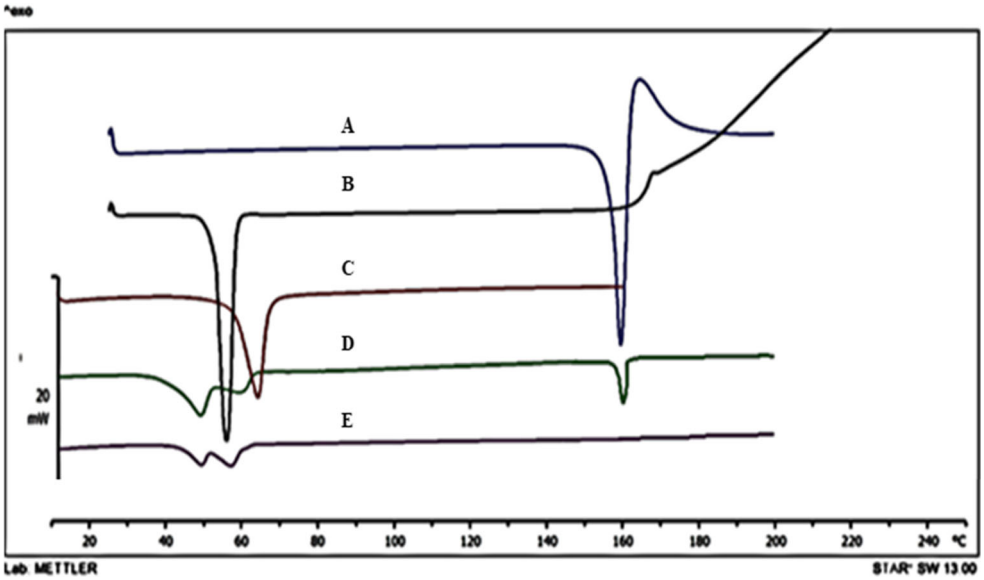

Fig. 11 DSC thermograms (A—free drug, B—Pluronic® F-127, C—GMS, D—physical mixture and E—NLC)

that small and isolated particles melt at temperatures much lower than the bulk [8, 26].

Powder X-ray diffraction

PXRD diffractograms of free drug, Pluronic® F-127, NLC are shown in the Fig. 12. The x-ray diffractograms of free IBR exhibited sharp intense peaks at 2θ values of 5.6°, 13.5°, 16.0°, 18.9°, 21.2° and 21.6° confirming the drug's crystal form. Pluronic® F-127 displays characteristic peaks at 18.9° band 23.5°. The characteristic peaks corresponding to IBR were absent and peaks corresponding to Pluronic® F-127 were seen in the diffractograms of NLC. This may be attributed to the conversion of the drug-loaded formulation into its amorphous counterpart [16].

In vitro drug release

Anticipating the slow release of drug from the dialysis bag, in vitro drug release study was performed up to 60 h as shown in Fig. 13. It was found that free drug suspension released about 98.68 ± 3.35% within 16 h while NLC released up to 67.41 ± 2.35 till 60 h. Since the free drug was in free suspension form, it had the greatest dissolution compared with NLC. The liquid lipid increases the permeability of nanoparticles to the surrounding media due to reduced density of packing provided by the matrix and pores created by the liquid lipid between the solid lipids. In vitro release data was subjected to various release kinetic equations to find the mechanism of drug release from the lipidic formulations. As shown in Table 4, data fitting was carried out by treating the in vitro release data into zero-order, first-order, Higuchi, Korsmeyer-Peppas, Hixon Crowell, Weibull and Bhaskar plots. For NLC, a good R^2 was obtained for zero-order, Peppas and Korsmeyer and Hixon Crowell kinetic models. Zero-order is the desired drug release which is a characteristic of lipidic formulations and the same was observed with optimised NLC batch. A good fit for Peppas and Korsmeyer indicates an anomalous non-Fickian ($n = 1$) release profile being a combination of both diffusion and erosion respectively. Interestingly, a good fit for Hixon Crowell equation indicates a diffusion release similar to powder type systems which may be attributed to uniform particulate sized NLC which present a uniform surface for the surrounding media, and the geometry of particles

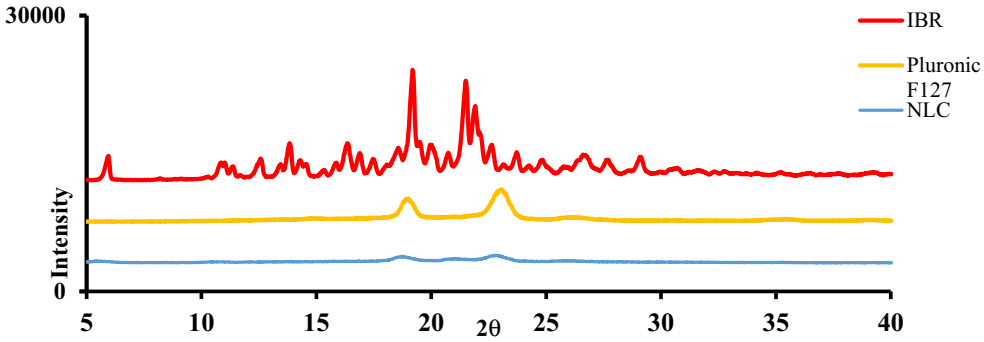

Fig. 12 PXRD diffractograms of free drug (IBR), Pluronic® F-127 and NLC

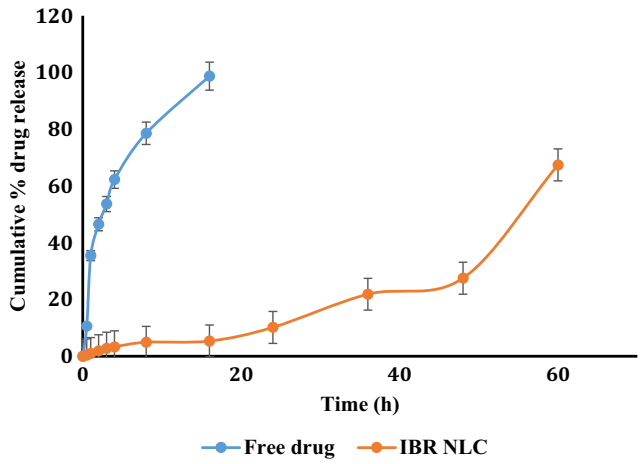

Fig. 13 In vitro drug release profile of free drug (Ibrutinib) and NLC (n = 3, data presented as mean ± SD)

remains unaffected throughout the drug release. This may be attributed to the presence of liquid lipid which causes imperfections in the solid lipid, and also, liquid lipid forms a layer around solid lipid increasing the diffusion of drug [57].

Stability studies

Stability is one of the most important aspects of any therapeutic formulation which warrants its safety and efficacy. Nanoformulations have a short shelf-life compared with the conventional; however, their proven efficacy had led them to gain importance. Stability studies of the optimised NLC were carried out at 4 °C and 25 °C. The results are depicted in Table 5 and the data was subjected to student's t test assuming unequal variances. Aliquots were acquired from the batches at the 0, 10th, 20th and 30th day intervals and evaluated for any changes in their particle size, PDI and entrapment efficiency respectively.

When NLC were stored at 4 °C, increase in particle size from 106.63 ± 8.66 to 114.42 ± 5.0 nm was obtained. While zeta potential of the optimised NLC batch on 0th day was found to be − 27.7 ± 3.34 mV and on the 30th day, it was about − 25.48 ± 5.45 mV. E.E. was also found to be reduced from 74.32 ± 5.52 to 67.28 ± 3.53%.

Storage at 25 °C showed an increase in particle size from 106.63 ± 8.66 to 120.62 ± 2.65 nm and an increase in PDI from 0.283 to 0.334. However, zeta potential and entrapment efficiency decreased significantly at the end of 30 days ($p < 0.05$). The liquid lipid may have reduced the Gibbs free energy barrier to a substantial amount for the formulation to be stable at 4 °C. By the reduction of Gibbs free energy, a more stable state, inhibiting solid-state transitions and polymorphic transformations, may be attained. E.E. of stability samples needs to be taken into consideration since drug leakage from nanostructured lipid carriers may not have significant impact on size but a statistically significant difference in E.E. was noticed. Hence, the suggested storage for NLC is 2–8 °C [57, 58].

Table 4 Release kinetics for in vitro drug release

	NLC	
	Equations	R^2
Zero order	$y = 4.1266x + 8.75$	0.90
First	$y = 0.077x + 0.97$	0.59
Higuchi	$y = 0.0612x + 0.13$	0.96
Korsmeyer-Peppas	$y = 1.2775x - 1.31$	0.89
Hixon Crowell	$y = -1.5129x + 3.18$	0.90
Weibull	$y = 0.037x - 2.06$	0.79
Bhaskar	$y = 1.256x + 2.11$	0.75

Pharmacokinetics

Bio-analytical method

HPLC method was developed and validated for parameters such as:

Specificity: chromatogram of sample and blank are compared and no interference was noticed.

Linearity/range: the ratio of peak area obtained with analyte to that of area of IS was plotted on Y-axis and concentration (ng/mL) on X-axis. The developed method was linear in the range 25 to 2000 ng/mL.

Sensitivity: the developed method was sensitive enough to have a limit of quantification 25 ng/mL.

Accuracy, precision and recovery results are shown in the supplementary Table 2. The values of accuracy and precision were well within the limits. Recovery of the method was consistent.

Animal studies

Plasma concentration-time profiles of the free drug and NLC were obtained and shown in Fig. 14. The pharmacokinetic parameters were calculated and shown in Table 6. Compared with the free drug, a significant increase in maximum concentration (C_{max}) (2.89-fold), area under curve ($AUC_{0\text{-}t}$) (5.32-fold) and mean residence time (MRT) (1.82-fold) were observed with NLC. The time taken to reach maximum concentration (t_{max}) was also found to be increased owing to the slow release of drug from the formulation. These results conclude a significant improvement in oral bioavailability of IBR via NLC compared with free drug.

Lymphatic uptake study by chylomicron flow blocking approach Traditionally evaluation of lymphatic transport was studied by a surgical model where lymphatic duct was

Table 5 Stability results of NLC ($n = 3$, data represented as mean ± SD)

Storage temperature	Day	Size (nm)	PDI	E.E. %	Zeta potential (mV)
4 °C	0	106.63 ± 8.66	0.28 ± 0.005	74.32 ± 5.52	− 27.7 ± 3.34
	10	110.20 ± 3.76	0.28 ± 0.003	71.82 ± 2.80	− 27.1 ± 4.24
	20	112.44 ± 6.07	0.28 ± 0.002	68.67 ± 1.69	− 26.95 ± 3.41
	30	114.42 ± 5.05	0.29 ± 0.002	67.28 ± 3.53	− 25.48 ± 5.45
25 °C	0	106.63 ± 8.66	0.28 ± 0.005	74.32 ± 5.52	− 27.70 ± 3.34
	10	112.26 ± 3.51	0.29 ± 0.007	69.74 ± 1.41	− 25.45 ± 5.67
	20	115.85 ± 4.08	0.30 ± 0.014	67.76 ± 2.80	− 24.12 ± 4.22
	30*	120.62 ± 2.65	0.33 ± 0.013	60.76 ± 1.38	− 18.63 ± 3.85

*Displayed statistical difference (p value < 0.05) in comparison with day 0

cannulated; this surgical procedure is preceded by lymphatic flow blocking approach. Later approach has no surgical procedures and does not interfere with other absorption pathways, and it has been proven to be equivalent to a surgical model. Owing to the advantages, this model is widely used to study the lymphatic uptake. The commonly used lymphatic flow blocker is cycloheximide, a protein synthesis inhibitor. It inhibits the production of chylomicrons and also inhibits the phagocytic activity of M cells thus blocking the lymphatic uptake of xenobiotics [8].

The equivalency of chylomicron flow block approach with that of surgical procedure was first established in male Wistar rats [47]; hence, in compliance with it, we have used male Wistar rats. However, similar studies were performed in rats of other strain, species and genders and similar results were reported [8, 59–61]. To compare the effect of CXI on the intestinal absorption, free drug in presence of CXI was also administered. The pharmacokinetic parameters C_{max}, $AUC_{0\text{-}t}$ and MRT of free drug in the absence of CXI were similar to that of the free drug in the presence of CXI, indicative of the absence of lymphatic uptake with the free drug. The results are further supported by previous reports which state that CXI only affects the lymphatic uptake and no other pathways. Additionally for a molecule to have inherent ability to undergo lymphatic uptake, it should possess log p value greater than 5 [13]. IBR has log P 3.97; hence, it did not show any inherent lymphatic uptake and formulating it with lipids can enhance the lymphatic uptake to avoid the first-pass effect.

On the other hand, the pharmacokinetic parameters of NLC administered in the presence of CXI were significantly inferior with that of NLC in the absence of CXI as shown in Fig. 14. C_{max}, $AUC_{0\text{-}t}$ and MRT of NLC without CXI were 2.75, 3.57 and 1.30 folds higher compared with NLC with CXI. Systemic entry of a xenobiotic from intestine occurs by portal vein or lymphatic transport. Blocking the lymphatic flow will cause the molecule to enter into portal circulation leading to first pass metabolism and resulting in low plasma concentrations, whereas in the absence of CXI, lymph production will not be altered and the xenobiotic can enter into lymph causing bypass of the first pass effect. This entry into lymphatic system causes the enhanced plasma concentration levels of the drug. From the results, it can be drawn that free drug cannot enter into lymph whereas the NLC can gain access into lymph and by pass the first pass effect. The enhancement of

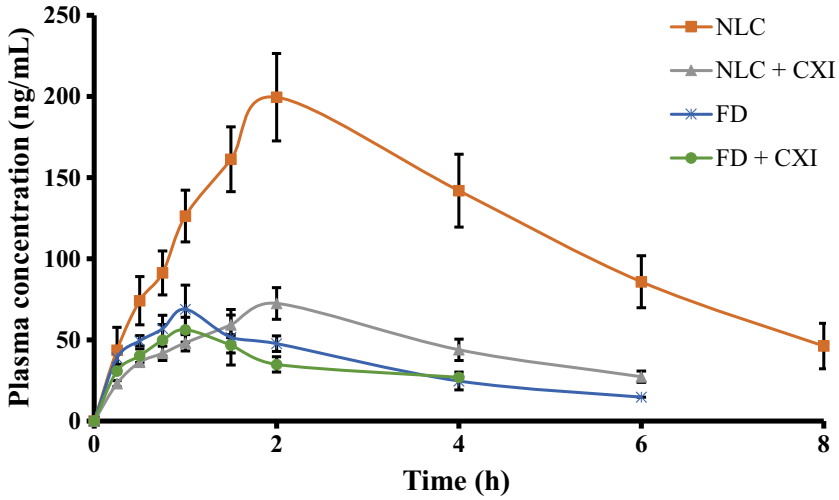

Fig. 14 Plasma concentration time profile of free drug (FD), free drug + cycloheximide (FD + CXI), NLC and NLC + cycloheximide (NLC + CXI) ($n = 6$, data presented as mean ± SD)

Table 6 Oral pharmacokinetics in rats ($n = 6$, data presented as mean ± SD)

Parameter	NLC	NLC + CXI	FD	FD + CXI
C_{max}	199.60 ± 25.60*	72.57 ± 16.91	68.97 ± 10.23	57.94 ± 14.53
Half-life (h)	6.34 ± 0.93*	5.19 ± 0.62	3.063 ± 0.79	2.607 ± 0.066
$AUC_{0\text{-}t}$ h*ng/mL	1107.71 ± 150.34*	309.88 ± 60.42	207.90 ± 59.24	175.81 ± 38.01
MRT (h)	4.32 ± 0.09*	3.30 ± 0.05	2.37 ± 0.11	2.38 ± 0.03

*Displayed statistical difference (p value < 0.05) in comparison with FD

pharmacokinetic parameters with formulation may be due to the orchestration of the triglyceride rich chylomicron secretion from the endoplasmic reticulum of intestinal cells. The secreted chylomicrons further sequestrate the entry of the NLC and facilitate the uptake through enterocytes into the mesenteric lymph nodes. Such transcellular mechanisms may occur anywhere across the intestinal epithelia [14, 46, 47]. Presence of lipids with a chain length greater than 14 carbons increases the lymphatic transport; in this study, GMS was used which contains 21 carbons. This long chain fatty acid might have caused increased lymphatic uptake [62]. The developed formulation had a zeta potential of − 27.7 mV; negative charge also increases the ability of formulations to get absorbed through the lymphatic route. As per literature, the lymphatic uptake of charged particles follows the order negative > positive > neutral [13]. Presence of Pluronic® F-127 might also contribute to enhanced bioavailability. As per previous reports, Pluronics® are known to deform intestinal cell membrane opening the tight junctions and enhancing the paracellular transport of formulations [57]. Through this study, we conclude the efficacy of NLC as a carrier system to improve the bioavailability of the drug by lymphatic uptake.

Conclusion

The selected solvent diffusion method was found to be suitable for the production of NLC. QbD was successfully applied for the development of IBR-loaded NLC. Screening for significant factors was performed by PBD; further optimisation was performed by CCD. The developed design was validated by various multi-variate analysis tools. FESEM and TEM analysis of the formulations showed spherical particles, DSC indicated the formation of molecular dispersion of drug in the melted lipid and PXRD results confirmed the amorphous transformation of the drug owing to the disappearance of the drug peaks from the diffractograms. In vitro, drug release studies had shown sustained release of drug from the formulation indicative of slow diffusion of the drug. In vivo pharmacokinetic study demonstrated a significant increase in oral bioavailability of the developed NLC formulation compared with free drug. Moreover, the lymphatic entry of the developed formulation was proven by chylomicron flow blocking approach.

Acknowledgements The authors are thankful to the NIPER-HYD and Department of Pharmaceuticals (DoP) for providing the facilities.

Compliance with ethical standards

Conflict of interest The authors declare that they have no conflict of interest.

Ethical statement All Institutional and National guidelines for the care and use of laboratory animals were followed.

References

1. Burger JA, Buggy JJ. Bruton tyrosine kinase inhibitor ibrutinib (PCI-32765). Leuk Lymphoma. 2013;54(11):2385–91.
2. Kokhaei P, Jadidi-Niaragh F, Sotoodeh Jahromi A, Osterborg A, Mellstedt H, Hojjat-Farsangi M. Ibrutinib-a double-edge sword in cancer and autoimmune disorders. J Drug Target. 2016;24(5):373–85.
3. Smith MR. Ibrutinib in B lymphoid malignancies. Expert Opin Pharmacother. 2015;16(12):1879–87.
4. Qiu Q, Lu M, Li C, Luo X, Liu X, Hu L, et al. Novel self-assembled ibrutinib-phospholipid complex for potently peroral delivery of poorly soluble drugs with pH-dependent solubility. AAPS PharmSciTech. 2018;19(8):3571–83.
5. Massó-Vallés D, Jauset T, Soucek L. Ibrutinib repurposing: from B-cell malignancies to solid tumors. Oncoscience. 2016;3(5–6):147.
6. Haura EB, Rix U. Deploying ibrutinib to lung cancer: another step in the quest towards drug repurposing. J Natl Cancer Inst. 2014;106(9):dju250.
7. Shakeel F, Iqbal M, Ezzeldin E. Bioavailability enhancement and pharmacokinetic profile of an anticancer drug ibrutinib by self-nanoemulsifying drug delivery system. J Pharm Pharmacol. 2016;68(6):772–80.
8. Makwana V, Jain R, Patel K, Nivsarkar M, Joshi A. Solid lipid nanoparticles (SLN) of Efavirenz as lymph targeting drug delivery system: elucidation of mechanism of uptake using chylomicron flow blocking approach. Int J Pharm. 2015;495(1):439–46.
9. Garg A, Bhalala K, Tomar DS. In-situ single pass intestinal permeability and pharmacokinetic study of developed Lumefantrine loaded solid lipid nanoparticles. Int J Pharm. 2017;516(1–2):120–30.
10. Xie S, Zhu L, Dong Z, Wang Y, Wang X, Zhou W. Preparation and evaluation of ofloxacin-loaded palmitic acid solid lipid nanoparticles. Int J Nanomedicine. 2011;6:547.

11. Gonçalves L, Maestrelli F, Mannelli LDC, Ghelardini C, Almeida A, Mura P. Development of solid lipid nanoparticles as carriers for improving oral bioavailability of glibenclamide. Eur J Pharm Biopharm. 2016;102:41–50.
12. Mishra DK, Dhote V, Bhatnagar P, Mishra PK. Engineering solid lipid nanoparticles for improved drug delivery: promises and challenges of translational research. Drug Deliv Transl Res. 2012;2(4): 238–53.
13. Khan AA, Mudassir J, Mohtar N, Darwis Y. Advanced drug delivery to the lymphatic system: lipid-based nanoformulations. Int J Nanomedicine. 2013;8:2733.
14. Kalepu S, Manthina M, Padavala V. Oral lipid-based drug delivery systems–an overview. Acta Pharm Sin B. 2013;3(6):361–72.
15. Nooli M, Chella N, Kulhari H, Shastri NR, Sistla R. Solid lipid nanoparticles as vesicles for oral delivery of olmesartan medoxomil: formulation, optimization and in vivo evaluation. Drug Dev Ind Pharm. 2017;43(4):611–7.
16. Shi X, Song S, Ding Z, Fan B, Huang W, Xu T. Improving the solubility, dissolution, and bioavailability of Ibrutinib by preparing it in a Coamorphous state with saccharin. J Pharm Sci. 2019;108: 3020–8.
17. Mehnert W, Mäder K. Solid lipid nanoparticles: production, characterization and applications. Adv Drug Deliv Rev. 2012;64:83–101.
18. Naseri N, Valizadeh H, Zakeri-Milani P. Solid lipid nanoparticles and nanostructured lipid carriers: structure, preparation and application. Adv Pharm Bull. 2015;5(3):305–13.
19. Beloqui A, del Pozo-Rodríguez A, Isla A, Rodríguez-Gascón A, Solinís MÁ. Nanostructured lipid carriers as oral delivery systems for poorly soluble drugs. J Drug Deliv Sci Technol. 2017;42:144–54.
20. Sahu AK, Kumar T, Jain V. Formulation optimization of erythromycin solid lipid nanocarrier using response surface methodology. Biomed Res Int. 2014;2014:1–8.
21. Lin C-H, Chen C-H, Lin Z-C, Fang J-Y. Recent advances in oral delivery of drugs and bioactive natural products using solid lipid nanoparticles as the carriers. J Food Drug Anal. 2017;25(2):219–34.
22. Radtke M, Müller RH. Nanostructured lipid drug carriers. New Drugs. 2001;2:48–52.
23. Müller RH, Alexiev U, Sinambela P, Keck CM. Nanostructured lipid carriers (NLC): the second generation of solid lipid nanoparticles. Percutaneous Penetration Enhancers Chem Methods Penetration Enhancement. Springer. 2016:161–85.
24. Nagaich U, Gulati N. Nanostructured lipid carriers (NLC) based controlled release topical gel of clobetasol propionate: design and in vivo characterization. Drug Deliv Transl Res. 2016;6(3):289–98.
25. Rangaraj N, Pailla SR, Chowta P, Sampathi S. Fabrication of ibrutinib nanosuspension by quality by design approach: intended for enhanced oral bioavailability and diminished fast fed variability. AAPS PharmSciTech. 2019;20(8):326.
26. Kaithwas V, Dora CP, Kushwah V, Jain S. Nanostructured lipid carriers of olmesartan medoxomil with enhanced oral bioavailability. Colloids Surf B: Biointerfaces. 2017;154:10–20.
27. Shah NV, Seth AK, Balaraman R, Aundhia CJ, Maheshwari RA, Parmar GR. Nanostructured lipid carriers for oral bioavailability enhancement of raloxifene: design and in vivo study. J Adv Res. 2016;7(3):423–34.
28. Negi LM, Jaggi M, Talegaonkar S. Development of protocol for screening the formulation components and the assessment of common quality problems of nano-structured lipid carriers. Int J Pharm. 2014;461(1–2):403–10.
29. Patwekar SL, Pedewad SR, Gattani S. Development and evaluation of nanostructured lipid carriers-based gel of isotretinoin. Part Sci Technol. 2018;36(7):832–43.
30. Natarajan J, Baskaran M, Humtsoe LC, Vadivelan R, Justin A. Enhanced brain targeting efficacy of olanzapine through solid lipid nanoparticles. Artif Cells Nanomed Biotechnol. 2017;45(2):364–71.
31. Wu P-S, Lin C-H, Kuo Y-C, Lin C-C. Formulation and characterization of hydroquinone nanostructured lipid carriers by homogenization emulsification method. J Nanomater. 2017;2017:1–7.
32. Singh B, Kapil R, Nandi M, Ahuja N. Developing oral drug delivery systems using formulation by design: vital precepts, retrospect and prospects. Expert Opin Drug Deliv. 2011;8(10):1341–60.
33. Kan S, Lu J, Liu J, Wang J, Zhao Y. A quality by design (QbD) case study on enteric-coated pellets: screening of critical variables and establishment of design space at laboratory scale. Asian J Pharm Sci. 2014;9(5):268–78.
34. Politis SN, Colombo P, Colombo G, Rekkas DM. Design of experiments (DoE) in pharmaceutical development. Drug Dev Ind Pharm. 2017;43(6):889–901.
35. Yerlikaya F, Ozgen A, Vural I, Guven O, Karaagaoglu E, Khan MA, et al. Development and evaluation of paclitaxel nanoparticles using a quality-by-design approach. J Pharm Sci. 2013;102(10): 3748–61.
36. Kovács A, Berkó S, Csányi E, Csóka I. Development of nanostructured lipid carriers containing salicyclic acid for dermal use based on the quality by design method. Eur J Pharm Sci. 2017;99:246–57.
37. Beg S, Saini S, Bandopadhyay S, Katare O, Singh B. QbD-driven development and evaluation of nanostructured lipid carriers (NLCs) of olmesartan medoxomil employing multivariate statistical techniques. Drug Dev Ind Pharm. 2018;44(3):407–20.
38. Mishra V, Kesharwani P, Amin MC, Iyer A, editors. Nanotechnology-Based Approaches for Targeting and Delivery of Drugs and Genes. Academic Press; 2017.
39. Xia D, Shrestha N, van de Streek J, Mu H, Yang M. Spray drying of fenofibrate loaded nanostructured lipid carriers. Asian J Pharm Sci. 2016;11(4):507–15.
40. Gupta B, Poudel BK, Tran TH, Pradhan R, Cho H-J, Jeong J-H, et al. Modulation of pharmacokinetic and cytotoxicity profile of imatinib base by employing optimized nanostructured lipid carriers. Pharm Res. 2015;32(9):2912–27.
41. Martins S, Tho I, Souto E, Ferreira D, Brandl M. Multivariate design for the evaluation of lipid and surfactant composition effect for optimisation of lipid nanoparticles. Eur J Pharm Sci. 2012;45(5):613–23.
42. Esbensen KH, Guyot D, Westad F, Houmoller LP. Multivariate data analysis: in practice: an introduction to multivariate data analysis and experimental design. Multivariate Data Analysis; 2002.
43. Baumgartner R, Teubl BJ, Tetyczka C, Roblegg E. Rational design and characterization of a nanosuspension for intraoral administration considering physiological conditions. J Pharm Sci. 2016;105(1):257–67.
44. Elmowafy M, Ibrahim HM, Ahmed MA, Shalaby K, Salama A, Hefesha H. Atorvastatin-loaded nanostructured lipid carriers (NLCs): strategy to overcome oral delivery drawbacks. Drug Deliv. 2017;24(1):932–41.
45. Sharma A, Jaiswal S, Shukla M, Sharma M, Chauhan PMS, Rangaraj N, et al. HPLC–MS-MS method development and validation of antileishmanial agent, S010-0269, in hamster serum. J Chromatogr Sci. 2015;53(9):1542–8.
46. Bhalekar MR, Upadhaya PG, Madgulkar AR, Kshirsagar SJ, Dube A, Bartakke US. In-vivo bioavailability and lymphatic uptake evaluation of lipid nanoparticulates of darunavir. Drug Deliv. 2016;23(7):2581–6.
47. Dahan A, Hoffman A. Evaluation of a chylomicron flow blocking approach to investigate the intestinal lymphatic transport of lipophilic drugs. Eur J Pharm Sci. 2005;24(4):381–8.
48. Zhang C, Peng F, Liu W, Wan J, Wan C, Xu H, et al. Nanostructured lipid carriers as a novel oral delivery system for

triptolide: induced changes in pharmacokinetics profile associated with reduced toxicity in male rats. Int J Nanomedicine. 2014;9: 1049.
49. Patel M, Sawant K. A quality by design concept on lipid based nanoformulation containing antipsychotic drug: screening design and optimization using response surface methodology. J Nanomed Nanotechnol. 2017;8(3):1–11.
50. Chouhan P, Saini T. D-optimal design and development of microemulsion based transungual drug delivery formulation of ciclopirox olamine for treatment of onychomycosis. Indian J Pharm Sci. 2016;78(4):498–511.
51. Patil-Gadhe A, Pokharkar V. Pulmonary targeting potential of rosuvastatin loaded nanostructured lipid carrier: optimization by factorial design. Int J Pharm. 2016;501(1–2):199–210.
52. Instruments M. Zetasizer nano series user manual. MAN0317. 2004;1:2004.
53. Singh A, Neupane YR, Panda BP, Kohli K. Lipid based nanoformulation of lycopene improves oral delivery: formulation optimization, ex vivo assessment and its efficacy against breast cancer. J Microencapsul. 2017;34(4):416–29.
54. Mandpe L, Pokharkar V. Quality by design approach to understand the process of optimization of iloperidone nanostructured lipid carriers for oral bioavailability enhancement. Pharm Dev Technol. 2015;20(3):320–9.
55. Su Y-L, Liu H-Z, Guo C, Wang J. Association behavior of PEO–PPO–PEO block copolymers in water or organic solvent observed by FTIR spectroscopy. Mol Simul. 2003;29(12):803–8.
56. Han L, Wang T. Preparation of glycerol monostearate from glycerol carbonate and stearic acid. RSC Adv. 2016;6(41):34137–45.
57. Tiwari R, Pathak K. Nanostructured lipid carrier versus solid lipid nanoparticles of simvastatin: comparative analysis of characteristics, pharmacokinetics and tissue uptake. Int J Pharm. 2011;415(1–2):232–43.
58. Das S, Ng WK, Tan RB. Are nanostructured lipid carriers (NLCs) better than solid lipid nanoparticles (SLNs): development, characterizations and comparative evaluations of clotrimazole-loaded SLNs and NLCs? Eur J Pharm Sci. 2012;47(1):139–51.
59. Liao H, Gao Y, Lian C, Zhang Y, Wang B, Yang Y, et al. Oral absorption and lymphatic transport of baicalein following drug–phospholipid complex incorporation in self-microemulsifying drug delivery systems. Int J Nanomedicine. 2019;14:7291–306.
60. Mishra A, Vuddanda PR, Singh S. Intestinal lymphatic delivery of praziquantel by solid lipid nanoparticles: formulation design, in vitro and in vivo studies. J Nanotechnol. 2014;2014:1–12.
61. Baheti A, Srivastava S, Sahoo D, Lowalekar R, Prasad Panda B, Kumar Padhi B, et al. Development and pharmacokinetic evaluation of industrially viable self-microemulsifying drug delivery systems (SMEDDS) for terbinafine. Curr Drug Deliv. 2016;13(1):65–75.
62. Trevaskis NL, Charman WN, Porter CJ. Lipid-based delivery systems and intestinal lymphatic drug transport: a mechanistic update. Adv Drug Deliv Rev. 2008;60(6):702–16.